Negative regulation of autoimmune demyelination by the inhibitory receptor CLM-1

Hongkang Xi,[1] Kenneth J. Katschke Jr.,[1] Karim Y. Helmy,[1] Paige A. Wark,[1] Noelyn Kljavin,[2] Hilary Clark,[3] Jeffrey Eastham-Anderson,[4] Theresa Shek,[5] Merone Roose-Girma,[2] Nico Ghilardi,[2] and Menno van Lookeren Campagne[1]

[1]Department of Immunology, [2]Department of Molecular Biology, [3]Department of Bioinformatics, [4]Department of Pathology, and [5]Department of Antibody Engineering, Genentech Inc., South San Francisco, CA 94080

Multiple sclerosis and its preclinical model, experimental autoimmune encephalomyelitis, are marked by perivascular inflammation and demyelination. Myeloid cells, derived from circulating progenitors, are a prominent component of the inflammatory infiltrate and are believed to directly contribute to demyelination and axonal damage. How the cytotoxic activity of these myeloid cells is regulated is poorly understood. We identify CMRF-35–like molecule-1 (CLM-1) as a negative regulator of autoimmune demyelination. CLM-1 is expressed on inflammatory myeloid cells present in demyelinating areas of the spinal cord after immunization of mice with MOG_{35-55} (myelin oligodendrocyte glycoprotein) peptide. Absence of CLM-1 resulted in significantly increased nitric oxide and proinflammatory cytokine production, along with increased demyelination and worsened clinical scores, whereas T cell responses in the periphery or in the spinal cord remained unaffected. This study thus identifies CLM-1 as a negative regulator of myeloid effector cells in autoimmune demyelination.

CORRESPONDENCE
Menno van Lookeren Campagne:
menno@gene.com

Abbreviations used: BMDC, BM-derived DC; CLM-1, CMRF-35–like molecule-1; CNS, central nervous system; DLN, draining LN; EAE, experimental autoimmune encephalomyelitis; ECD, extracellular domain; ITIM, immunoreceptor tyrosine-based inhibition motif; MOG_{35-55}, myelin oligodendrocyte glycoprotein; mRNA, messenger RNA; T reg, regulatory T.

Myeloid cell–mediated destruction of myelin sheets and axons is thought to be the primary mechanism leading to loss of motor function in multiple sclerosis and experimental autoimmune encephalomyelitis (EAE; Benveniste, 1997). The myeloid effector populations in the central nervous system (CNS) consist of resident activated microglia and blood-derived mononuclear cells including monocytes, macrophages, and DCs. A subpopulation of the infiltrating myeloid cells expresses CD11c, MHC class II, and CD86 and is often referred to as CNS DCs (Deshpande et al., 2007). These effector cells have been shown to reactivate antigen-specific T cells (Bailey et al., 2007; Deshpande et al., 2007) and are involved in epitope spreading resulting in a remitting-relapsing disease course (Miller et al., 2007). In addition to serving as antigen-presenting cells, CNS-infiltrating $CD11c^+$ inflammatory myeloid cells also display T cell–independent effector functions through secretion of proinflammatory cytokines and reactive oxygen intermediates that can directly contribute to progressive demyelination and axon loss (Dogan et al., 2008; King et al., 2009).

CMRF-35–like molecule-1 (CLM-1; also named MAIR-V, LMIR3, DigR2) is a member of the CD300 family of receptors, a multigene cluster of type I transmembrane glycoproteins with a single extracellular IgV domain on human chromosome 17 and mouse chromosome 11 (Márquez et al., 2007; Clark et al., 2009). Two receptors in this cluster (CLM-1 and CLM-8) contain an immunoreceptor tyrosine-based inhibition motif (ITIM) in their intracellular domains, whereas the remainder of the receptor family carries charged residues in the transmembrane region that serve to recruit signaling adapters. CLM-1, the mouse orthologue of human CD300f (Clark et al., 2009), was first described as a negative regulator of osteoclastogenesis in vitro (Chung et al., 2003). Subsequent in vitro studies have confirmed that CLM-1, or its human orthologue CD300f

Paige A. Wark's present address is the University of British Columbia, Vancouver, British Columbia V6T 1Z4, Canada.

The Rockefeller University Press $30.00
J. Exp. Med. Vol. 207 No. 1 7-16
www.jem.org/cgi/doi/10.1084/jem.20091508

(also named IREM-1), serves as an inhibitory receptor in myeloid cells (Alvarez-Errico et al., 2004; Fujimoto et al., 2006; Izawa et al., 2007, 2009). One study finds that CLM-1 mediates caspase-independent cell death upon cross-linking with antibodies (Can et al., 2008). So far, a biological role in autoimmune disease has not been described. In this paper, we show that CLM-1 is expressed on iNOS- and TNF-producing inflammatory myeloid cells that invade the spinal cord after myelin oligodendrocyte glycoprotein (MOG_{35-55}) immunization. We further demonstrate that CLM-1 acts as a negative regulator of myeloid cell activity in vivo by suppressing the release of inflammatory cytokines and reactive oxygen species. This study thus identifies CLM-1 as a myeloid-specific negative regulator of CNS inflammation and demyelination.

RESULTS AND DISCUSSION

CLM-1 is expressed on BM-derived CD11c$^+$ cells at sites of CNS inflammation

A genome-wide search was performed to identify single transmembrane Ig superfamily members containing an ITIM (Yu et al., 2009). Mouse homologues of the candidate ITIM-containing genes were then selected based on their specific expression on myeloid cells and expression levels in the spinal cord after immunization with MOG_{35-55} peptide. Of all candidate ITIM genes, CLM-1 messenger RNA (mRNA) levels showed the highest fold increase (>1,500-fold) relative to naive mice at 2 wk after immunization (Fig. 1 A). Monoclonal antibodies to CLM-1 extracellular domain (ECD) were generated to determine the cellular source of CLM-1. CLM-1 was absent on the CD11b$^+$ local microglia population in naive mice (Fig. 1 B, left). In spinal cords from MOG-immunized mice, CLM-1 was highly expressed on CD11b$^+$CD11c$^+$ myeloid cells that also expressed MHC class II, CD86, and Gr-1 (Fig. 1 B, right; and Fig. S1 B). Immunohistochemical studies further illustrated that CLM-1$^+$CD11c$^+$ cells appear in clusters located predominantly in the ventrolateral funiculi of the cervical spinal cord (Fig. 1 C). Although CNS-resident CD45^{lo}CD11b$^+$CD11c$^-$ microglia cells did not express CLM-1 and iNOS and expressed low levels of TNF, CD45^{hi}CD11b$^+$ BM-derived myeloid cells present in spinal cord at the onset and peak of disease expressed CLM-1, iNOS, and TNF (Fig. 1 D). A subset of CLM-1$^+$ cells also expressed CD11c and, therefore, displayed characteristics of the TNF- and iNOS-producing (Tip) DCs that were originally described by Serbina et al. (2003).

We next determined the origin of the CLM-1$^+$ cells present in the inflamed spinal cord. Because CNS-resident microglia can transform into cells with DC-like characteristics after immune stimulation (Fischer and Reichmann, 2001), we determined if the CLM-1–positive cells in the inflamed CNS derive from irradiation-sensitive hematopoietic cells or from irradiation-resistant CNS-resident microglia. Mice bearing the allotypic CD45.1 marker were irradiated and reconstituted with BM cells from donor mice with the CD45.2 allotype. Consistent with the lack of CLM-1 expression on resident microglia in the naive spinal cord, CLM-1 was absent on irradiation-resistant myeloid cells but present on BM-derived donor cells in the inflamed CNS tissue (Fig. 2 A).

Circulating Ly6C^{hi}CD11b$^+$ inflammatory monocytes have been identified as precursors of CD11c$^+$ DCs present in the spinal cord of MOG_{35-55}-immunized mice (Dogan et al., 2008). GM-CSF–induced recruitment of the inflammatory Ly6C^{hi} monocytes from BM immediately before clinical manifestation of disease is paralleled by increased disease severity in EAE (King et al., 2009), indicating that the Ly6C^{hi} monocytes are candidate precursors of CNS-infiltrating cells with cytotoxic function. The inflammatory monocyte population can be distinguished from resident noninflammatory monocytes based on their expression levels of CX_3CR1 (Geissmann et al., 2003; Auffray et al., 2009b). To determine which myeloid cell subset expresses CLM-1, we used $CX_3CR1^{GFP/+}$ mice in which one allele for the gene encoding CX_3CR1 has been replaced with the gene encoding GFP, resulting in GFP labeling of all cells from the monocyte/DC/macrophage lineage including microglia (Geissmann et al., 2003). In peripheral blood, CLM-1 was expressed on CX_3CR1^{lo}Ly6C^{hi}CD115$^+$CD62L$^+$Ly6G$^-$ inflammatory monocytes (Geissmann et al., 2003; Auffray et al., 2009a) before disease onset but was absent on CX_3CR1^{hi}-resident monocytes in both naive and immunized mice (Fig. 2 B and Fig. S1 C). This suggests that CLM-1 is associated with inflammatory monocytes that act as precursors of cytotoxic CD11c$^+$ cells in the spinal cord. In the CNS, consistent with the expression of CX_3CR1 on infiltrating myeloid cells (Sunnemark et al., 2005), CLM-1$^+$$CX_3CR1^{lo}$ cells were found adjacent to the leptomeningeal vessels of the thoracic spinal cord on day 14 after immunization, whereas CX_3CR1^{hi} ramified microglia cells, which are primarily located in the gray matter of the spinal cord, did not express CLM-1 (Fig. 2, C and D). Based on these observations, we hypothesized that CLM-1 may regulate pathological responses of CNS-infiltrating myeloid effector cells but not of CNS-resident microglial cells in MOG_{35-55}-induced EAE.

Absence of CLM-1 results in increased disease severity in MOG35–55–induced EAE

Based on the expression of CLM-1 on inflammatory monocytes and CNS-infiltrating CD11c$^+$ cytotoxic effector cells, we next determined if CLM-1 acts to attenuate myeloid cell–mediated inflammatory responses in MOG_{35-55}-induced EAE. Mice were generated in which exon 1 of CLM-1 was deleted through homologous recombination (Supplemental material and Fig. S2 A). Successful ablation of the CLM-1 gene in KO mice was confirmed by PCR (Fig. S2 B), Western blot analysis of BM-derived DCs (BMDCs; Fig. 3 A), and flow cytometry (Fig. 3 B) and immunohistochemistry (Fig. 3 C) analyses of CD11b$^+$CD11c$^+$ cells isolated from inflamed spinal cord. CLM-1 KO mice were viable and born in the expected Mendelian ratios. Mice did not differ in weight or bone parameters measured at 6 wk of age (unpublished data). Numbers of myeloid and lymphoid cell subsets in the inguinal LNs, spleens, and blood were similar in

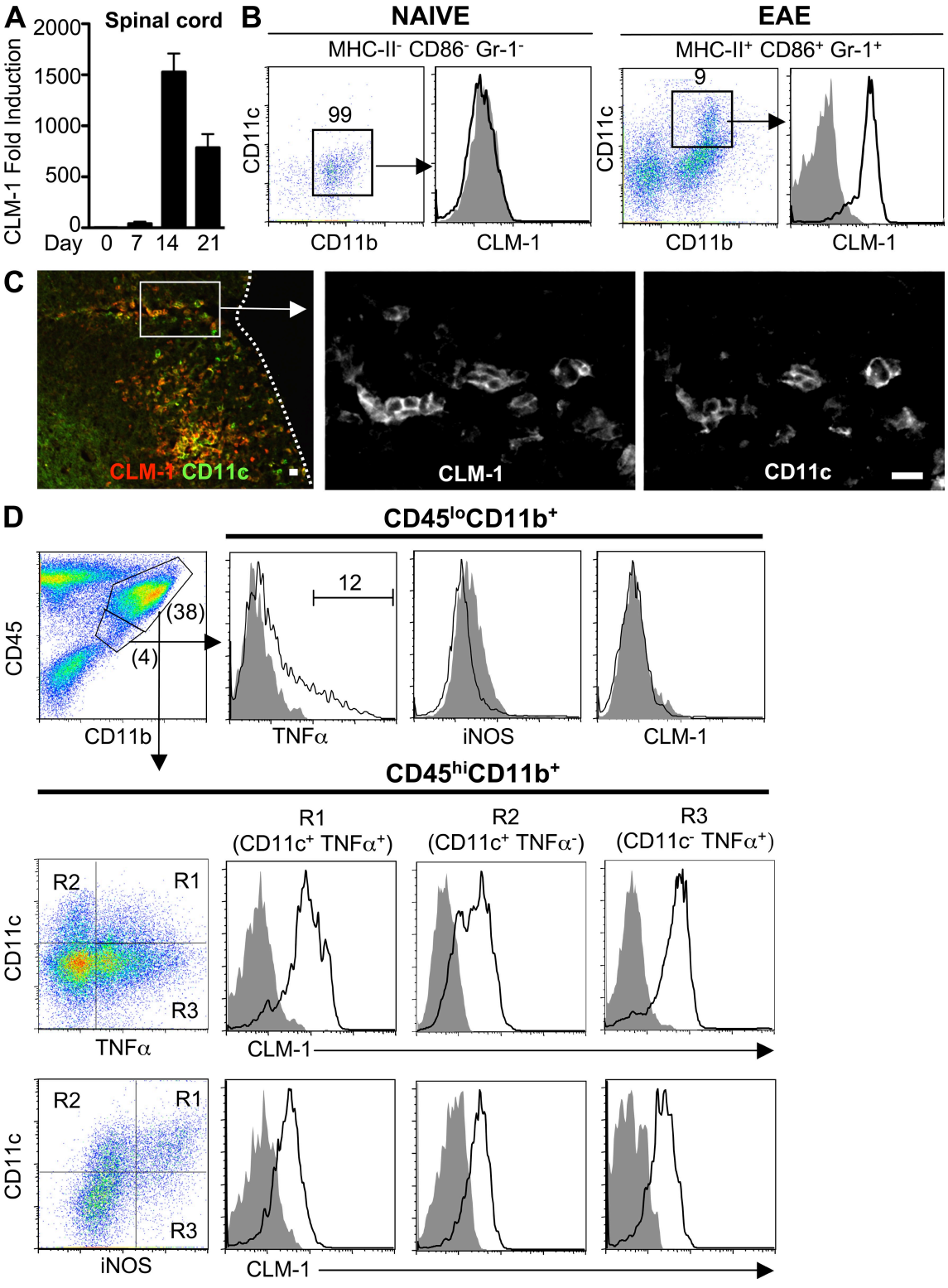

Figure 1. CLM-1 is expressed on myeloid cells in CNS inflammatory lesions. (A) CLM-1 mRNA expression in spinal cord after MOG_{35-55} immunization. Fold induction is calculated based on day 0 values. Values are expressed as means ± SEM. (B) CLM-1 expression on $CD11b^+CD11c^+$ cells in the spinal cord of naive and MOG_{35-55}-immunized mice. (C) Clusters of CLM-1^+ $CD11c^+$ myeloid cells in the ventrolateral funiculi and adjacent to leptomeninges (dotted line) of the cervical spinal cord (rectangle enlarged in middle and right). Bar, 10 µm. (D) TNF, iNOS, and CLM-1 expression on $CD45^{lo}CD11b^+$-resident microglia (top row) and on $CD45^{hi}CD11b^+$-infiltrating BM-derived cells. Open histograms represent antigen-specific staining and shaded histograms represent isotype control. Results shown are from one experiment out of three, with five (A), three (C), or two (B and D) mice per experimental group.

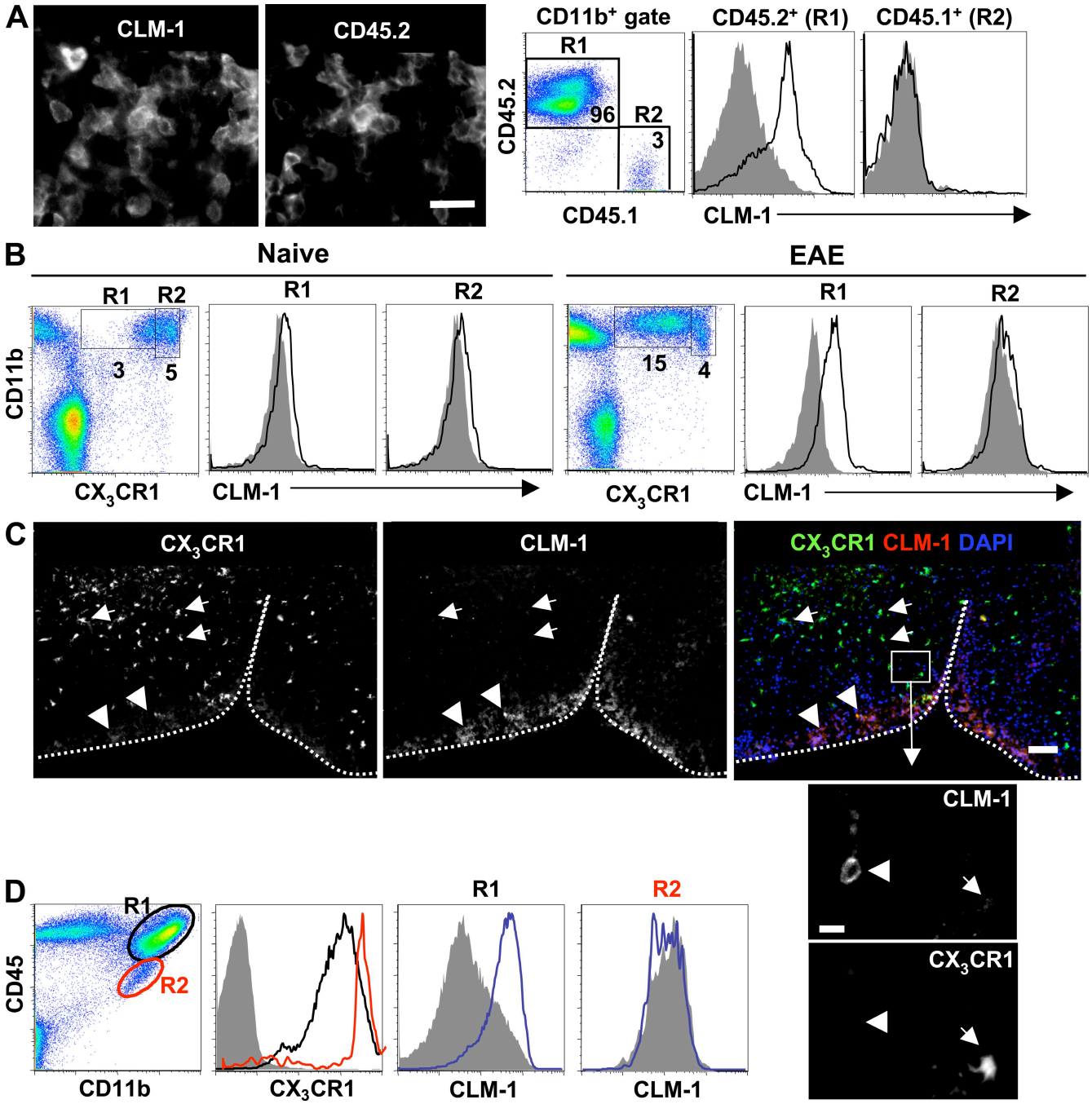

Figure 2. CLM-1 expression on irradiation-sensitive myeloid cells infiltrating the CNS and on inflammatory monocytes in the circulation. (A) CLM-1 expression on recipient (CD45.1$^+$) or donor (CD45.2$^+$)-derived myeloid cells as determined by immunohistochemistry (left) and flow cytometry (right). (B) CLM-1 expression on $CX_3CR1^{lo}CD11b^+$ inflammatory monocytes and $CX_3CR1^{hi}CD11b^+$-resident monocytes 7 d after MOG_{35-55} immunization. (C) CX_3CR1 and CLM-1 expression in a thoracic spinal cord section 14 d after immunization. CX_3CR1^{lo}CLM-1$^+$ cells are localized in the ventromedian funiculi (arrowheads) close to the leptomeninges (dotted line). CX_3CR1^{hi}CLM-1$^-$ cells (arrows) are present throughout the white and gray matter of the ventral horn. Enlarged views of the rectangle show nonoverlapping staining of CLM-1 on a cell with a dendritic-like morphology and high CX3CR1-GFP expression on a ramified microglia cell. (D) CLM-1 expression on $CD45^{hi}CX3CR1^{lo}$ BM-derived myeloid cells and $CD45^{lo}CX3CR1^{hi}$ microglia. Open histograms in A, B, and D represent antigen-specific staining and shaded histograms represent isotype controls. Results shown are from one experiment out of two (A and C) or three (B and D), with four (A) or two (B–D) mice per experimental group. Bars: (A and enlarged views in C) 10 µm; (C) 100 µm.

CLM-1 KO and WT mice (unpublished data), indicating that CLM-1 absence does not influence the rate of cellular turnover. Expression levels of cell surface molecules associated with antigen presentation and costimulation were similar on $CD11b^+CD11c^+$ cells isolated from CLM-1 WT and KO spinal cords at the peak of disease (Fig. S2 C). Expression levels of other members of the CMRF cluster were similar in resting and LPS-stimulated BMDCs derived from

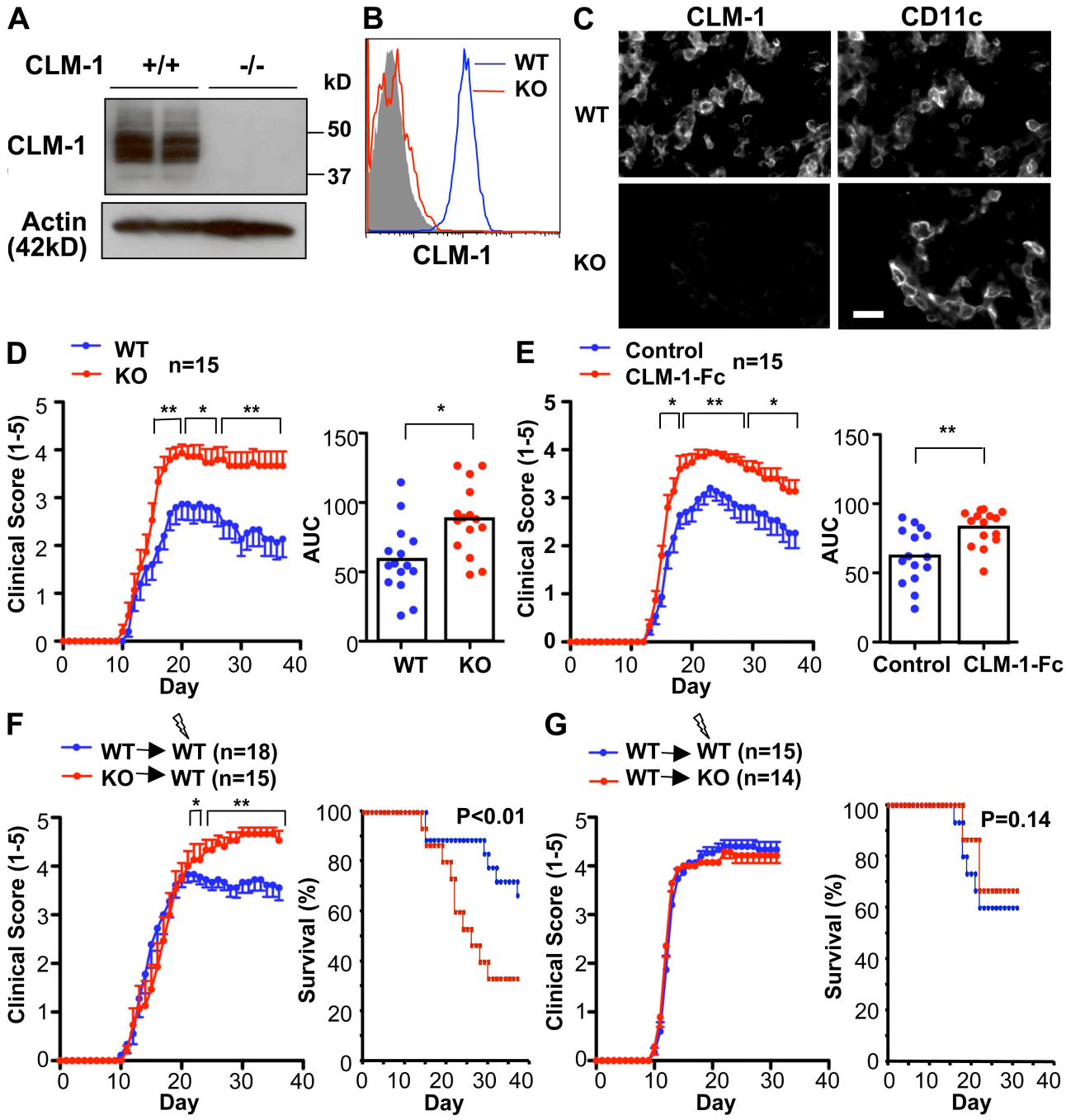

Figure 3. Lack of CLM-1 on BM-recruited cells or treatment with a CLM-1-Fc fusion protein increases EAE disease severity. (A) CLM-1 protein expression in BMDCs obtained from CLM-1 WT and KO mice. (B) Surface-expression of CLM-1 on $CD11c^+$ myeloid cells isolated from inflamed spinal cords of CLM-1 WT and KO mice. Shaded histograms represent isotype control. (C) CLM-1 staining on $CD11c^+$ myeloid cells in inflamed spinal cords from WT and KO mice. Bar, 10 µm. (D) Clinical scores in CLM-1 WT and KO mice. (E) Clinical scores in WT mice treated with CLM-1-Fc or control fusion protein. (F and G) Clinical scores and mortality in irradiated chimeras consisting of CLM-1 WT or KO mice reconstituted with BM cells from CLM-1 WT or CLM-1 KO mice. Results shown in A–C are from one of two experiments with two mice per group. Values shown in D–G are means ± SEM from one experiment out of three (D and E) or two (F and G) with 14–18 mice per group. *, $P < 0.05$; **, $P < 0.01$. AUC, area under curve.

CLM-1 WT and KO mice (Fig. S2, D and E). Disease incidence was comparable in CLM-1 WT and KO mice upon MOG_{35-55} immunization (Fig. S3 A). However, disease severity was significantly increased in mice lacking CLM-1 (Fig. 3 D). To determine if the protective role of CLM-1 in EAE is regulated by the interaction of CLM-1 ECD with a putative ligand, mice were treated with a soluble ectodomain of CLM-1 (CLM-1-Fc). Similar to the results obtained in CLM-1 KO mice, disease incidence was comparable (Fig. S3 B) but disease severity was significantly increased in CLM-1-Fc–treated mice as compared with mice treated with a control fusion protein (Fig. 3 E). These results suggest that CLM-1 is a negative regulator of CNS inflammation, potentially through interaction of the CLM-1 ECD with a putative ligand. BM chimeras were established to determine whether the increased disease severity was a result of the absence of CLM-1 on irradiation-sensitive BM-infiltrating cells as opposed to irradiation-resistant microglia. CLM-1 WT mice reconstituted with BM from KO mice showed similar disease incidence but increased disease severity compared with WT mice reconstituted with BM from WT mice (Fig. 3 F and Fig. S3 D). In contrast, KO mice reconstituted with BM from WT mice showed disease severity similar to that in WT recipients reconstituted with WT BM (Fig. 3 G and Fig. S3 E). Thus, absence of CLM-1 on a population of inflammatory BM-derived myeloid cells, but not microglia, increases disease severity in EAE.

CLM-1 does not modulate disease-initiating T cell responses

Because EAE is initiated and driven by antigen-specific $CD4^+$ T cells, we further determined if CLM-1 influences disease progression through its regulation of effector T cell responses in vitro and in vivo. Splenic DCs or BMDCs derived from CLM-1 WT and KO mice were incubated with allogeneic $CD4^+$ T cells or with $CD4^+$ T cells expressing a TCR specific for OVA peptide. T cell proliferation (Fig. S4, A–D) and cytokine responses (Fig. S4 E), as determined in this in vitro assay, did not depend on CLM-1 status. To further determine if CLM-1 influences T cell priming ex vivo, $CD4^+$ T cells isolated from draining LNs (DLNs) 7 d after MOG_{35-55} immunization were isolated and restimulated with MOG_{35-55} peptide. CLM-1 absence did not significantly alter T cell proliferation (Fig. 4 A), generation of $Foxp3^+$ regulatory T (T reg) cells (Fig. 4 B and Fig. S4 F), or T cell cytokine responses (Fig. 4 C). Finally, to probe a potential role for CLM-1 in regulating T cell effector functions in vivo, encephalitogenic $CD4^+$ T cells isolated from DLNs of CLM-1 WT and KO donor mice at 10–12 d after MOG_{35-55} immunization were adoptively transferred into KO and WT recipients. Disease severity was not influenced by CLM-1 status of the T cell donor (Fig. 4 D and Fig. S3 F) but was significantly enhanced in T cell recipients lacking CLM-1 (Fig. 4 E and Fig. S3, G and H). This indicates that CLM-1 acts to regulate disease severity at the effector phase, but not the T cell–priming phase, of the disease after MOG_{35-55} immunization.

Increased myeloid cell activation and demyelination in mice lacking CLM-1

Next, we determined whether CLM-1 influenced reactivation of CNS-infiltrating $CD4^+$ T cells. Spinal cord leukocytes harvested from CLM-1 WT and KO mice at the peak of disease and restimulated with MOG_{35-55} showed similar polarization toward Th1, Th17, and $Foxp3^+$ T reg cells and similar T cell–specific cytokine responses (Fig. 5 A, top row; and Fig. S4 G). In contrast, leukocytes harvested from spinal cords of CLM-1 KO mice produced significantly elevated levels of nitric oxide and myeloid-specific proinflammatory cytokines as compared with WT mice (Fig. 5 A, bottom row). Thus, CLM-1 negatively regulates local myeloid effector function in the CNS without affecting T cell responses. Because microglia do not express CLM-1 and iNOS, and given the relatively small (~10%) contribution of microglia to the total myeloid cell population harvested from the CNS at day 15 after MOG immunization, it seems likely that the increased NO_2^- and myeloid proinflammatory cytokine production is contributed by the infiltrating myeloid cells and not by microglia.

Increased production of reactive nitrogen species and release of proinflammatory cytokines by myeloid cells has been implicated in demyelination in EAE and multiple sclerosis (Hooper et al., 1997; Dogan et al., 2008). Therefore, we further determined if enhanced cytotoxic activity of myeloid cells in the spinal cord leads to increased demyelination. CLM-1–positive cells were found clustered at sites of demyelination in the dorsal and ventral funiculi of the cervical and thoracic spinal cord. The cells were found apposed to, and often wrapped around, myelin sheets with, in some cases, MOG-positive myelin remnants present inside CLM-1–positive cells (Fig. 5 B). Consistent with a role of CLM-1 in reducing myeloid effector responses, lack of CLM-1 resulted in increased demyelination (Fig. 5, C and D; and Fig. S3, C, H, and I), whereas numbers of infiltrating leukocytes remained unaltered (Fig. 5 E). Thus, CLM-1 negatively regulates myeloid cell activation in the inflamed spinal cord.

Even though the identification of receptors expressed by genes in the CMRF/CD300 gene cluster has been completed (Clark et al., 2009), their biological role is still poorly understood. For the first time, this study identifies CLM-1 as a negative regulator of myeloid effector cells recruited from peripheral blood to the CNS after MOG immunization (Dogan et al., 2008; King et al., 2009). The characterization of CLM-1 as an inhibitory receptor in vivo is consistent with previous in vitro studies (Chung et al., 2003; Alvarez-Errico et al., 2004; Izawa et al., 2007) that have demonstrated a role for the cytoplasmic ITIM domain of CLM-1 and its human orthologue CD300f in recruiting SHP-1 (Src homology-2 domain-containing protein tyrosine phosphatases-1), in turn inhibiting cellular effector responses.

Although cross-linking of the receptor with antibodies may reveal some aspects of CLM-1/CD300f signaling (Alvarez-Errico et al., 2007; Can et al., 2008; Izawa et al., 2009), identification of a natural ligand will be crucial to understand

CLM-1 biology and may potentially lead to identification of a therapeutic for treatment of autoimmune demyelinating diseases. Our results suggest that CLM-1 interacts with a putative ligand to modulate myeloid effector function in the CNS. Treatment with a soluble version of the receptor increases disease severity in EAE, phenocopying the CLM-1 KO mouse. One explanation for this is that the recombinant soluble receptor competitively inhibits the binding of a ligand that activates CLM-1, thus preventing down-modulation of immune responses in the immune-privileged CNS. Previous studies have demonstrated binding of a CLM-1 spliced variant, DigR2, to a putative ligand on T cells resulting in negative regulation of T cell responses (Shi et al., 2006). In various assays, we have not been able to detect binding of CLM-1 ECD to T cells, which is compatible with our results showing that T cell responses in vitro and in vivo are independent of CLM-1 expression on antigen-presenting cells. The different findings in our paper compared with the previous paper may be explained by the presence of a 7-aa insertion in the ECD of DIgR2 introduced by alternative splicing.

A subset of the CLM-1–expressing myeloid cells in the CNS resembles iNOS and TNF-producing myeloid effector cells recruited to the spleen after infection with the intracellular pathogen *Listeria monocytogenes* (Serbina et al., 2003). We therefore tested if CLM-1 regulates bactericidal activity of myeloid cells toward *L. monocytogenes*. No significant differences were found in live pathogen counts in spleens of CLM-1 WT and KO mice at 1, 2, or 6 d after intravenous injection of the pathogen (unpublished data), indicating that CLM-1 does not influence myeloid cell–driven innate immune responses toward *L. monocytogenes*.

Together, our study demonstrates that CLM-1 plays a nonredundant role in controlling myeloid cell activation and CNS demyelination. We further demonstrate that $CD11c^+$ inflammatory myeloid cells infiltrating the CNS can affect disease progression in the absence of altered T cell responses.

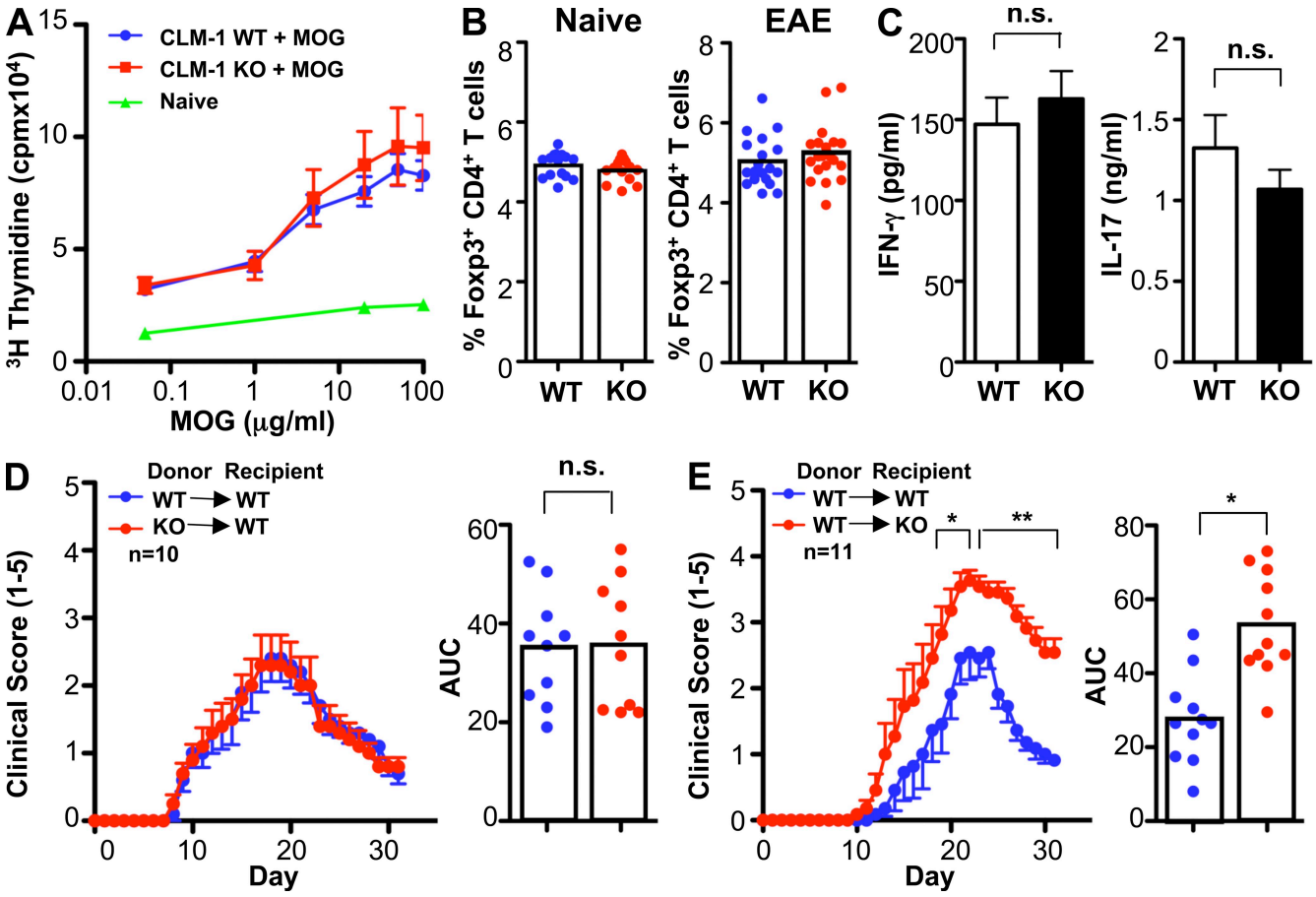

Figure 4. CLM-1 absence increases disease severity without affecting T cell priming. (A) T cells isolated from DLNs 7 d after immunization were restimulated with MOG_{35-55} peptide and proliferation was measured by ^{3}H thymidine incorporation. (B) Quantification of Foxp3-expressing $CD4^+$ T cells obtained from DLNs of naive CLM-1 WT and KO mice or 14 d after immunization. (C) Cytokine responses of $CD4^+$ T cells obtained from MOG_{35-55}-immunized mice restimulated with MOG_{35-55} peptide ex vivo. (D) Adoptive EAE by transfer of encephalitogenic $CD4^+$ T cells isolated from DLNs of CLM-1 WT or KO mice into CLM-1 WT recipients. (E) Adoptive EAE by transfer of encephalitogenic $CD4^+$ T cells isolated from DLNs of CLM-1 WT mice into CLM-1 WT or KO recipients. Values are expressed as means ± SEM and experiments have been repeated three times with 6 (A and C), 15–18 (B), 10 (D), and 11 (E) mice per group. n.s., not significant. *, $P < 0.05$; **, $P < 0.01$. AUC, area under curve.

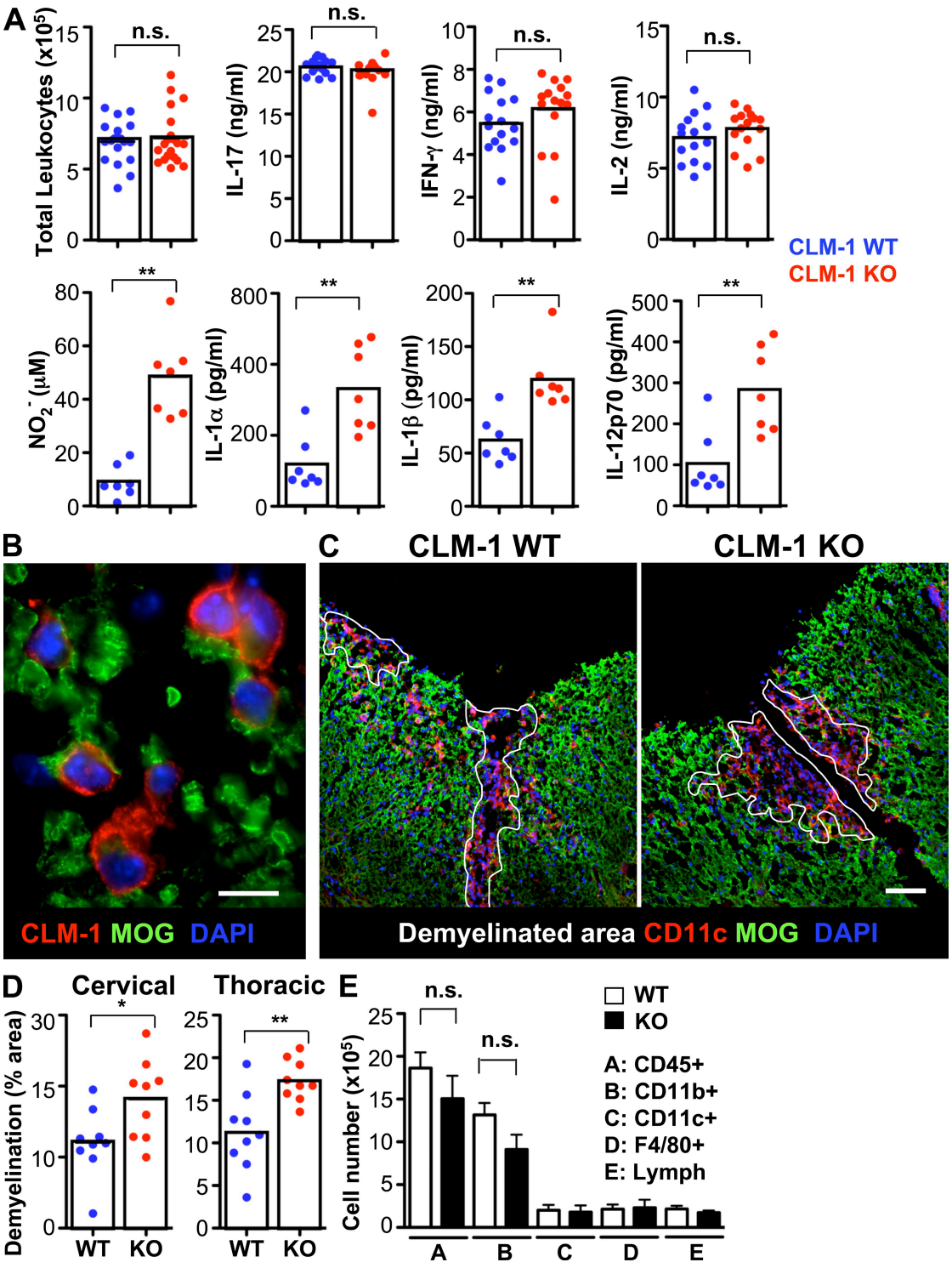

Figure 5. Lack of CLM-1 results in increased release of myeloid-specific inflammatory mediators and exacerbated demyelination. (A) Production of Th1, Th17, and myeloid cell–specific cytokines by leukocytes isolated from spinal cord 15 d after immunization. (B) CLM-1–positive cells apposed to MOG-positive myelin in the dorsal funiculus of the thoracic spinal cord on day 15 after immunization. (C) MOG and CD11c staining in the dorsal funiculus of the thoracic spinal cord on day15 after immunization. The lines delineate the area of demyelination. (D) Quantification of demyelinated regions in CLM-1 WT and KO mice. (E) Quantification of infiltrating leukocytes in the spinal cords of WT and KO mice 15 d after MOG immunization. Values in E are expressed as means ± SEM of six mice per group. Each symbol represents one individual mouse (A [top row] and D) or a pool of two to three mice (A, bottom row). Experiments were repeated twice (A–D) or three times (E) with at least six mice per group. n.s., not significant. *, $P < 0.05$; **, $P < 0.01$. Bars: (B) 10 µm; (C) 50 µm.

MATERIALS AND METHODS

Animals. All animals were held under sterile pathogen-free conditions and animal experiments were approved by the Institutional Animal Care and Use Committee of Genentech, Inc. CLM-1 KO mice were generated as described in Fig. S2. C57BL/6 mice on a CD45. 1 or CD45.2 congenic background and DO11.10 T cell transgenic mice were purchased from The Jackson Laboratory. $CX_3CR1^{gfp/+}$ C57BL/6 reporter mice were generated as previously described (Geissmann et al., 2003).

Antibodies and recombinant proteins. All antibodies were purchased from BD with the following exceptions: Pacific blue anti-CD11b (M1/70), PE-Cy7 anti-CD11c (N418), PE-Cy5 anti-I-A/I-E (M5/114.15.2), APC–Alexa Fluor 750 anti-F4/80 (BM8), and APC anti-CD115 (AFS98; eBioscience); streptavidin Pacific orange (Invitrogen); PE donkey anti–rabbit IgG and Cy3 anti–hamster IgG (Jackson ImmunoResearch Laboratories); and monoclonal anti-actin antibody (AC-40; Sigma-Aldrich). CLM-1-Fc fusion protein was generated by ligating the ECD (aa 1–176) of mouse CLM-1 to the mouse IgG1 Fc portion using a modified pRK5 expression vector. CLM-1-Fc fusion protein expressed in CHO cells was purified by protein A affinity chromatography and Superdex 200 gel filtration and the sequence verified by mass spectrometry analysis. The endotoxin level was <0.05 EU/mg. Monoclonal antibodies to the ECD of mouse CLM-1 were generated by immunizing Armenian hamsters with mouse CLM-1-ECD-His fusion protein. Splenic B cells from immunized animals were fused to myelomas to generate clone 3F6, which produces monoclonal antibodies selective for CLM-1 (no cross-reactivity to CLM-5). Alexa fluorochrome (488 or 647)–conjugated CLM-1 antibodies were generated using the Alexa Fluor protein labeling kit (Invitrogen).

MOG_{35-55}-induced EAE. Immunization and clinical scoring of CLM-1 WT and KO mice was performed as previously described (Batten et al., 2006). 200 µg CLM-1-Fc fusion protein or control protein (anti-gp120, mouse IgG1 isotype) in 100 µl PBS was injected subcutaneously three times per week starting on day 0 of immunization. Serum levels of CLM-1-Fc were 19 ± 5 µg/ml (mean ± SD) at the termination of the study.

BM chimeras. 6-wk-old C57BL/6 (CD45.1) recipient mice were irradiated with two doses of 500 rad and received BM from C57BL/6 (CD45.2) donor mice. EAE was induced 8 wk later when 80–100% (depending on cell type) reconstitution was achieved.

Adoptive transfer of EAE. 10–12 d after immunization, inguinal and brachial DLNs were harvested from CLM-1 WT or KO mice. Cells were restimulated for 4 d with MOG_{35-55} peptide in RPMI 1640 medium with 20 ng/ml recombinant mouse IL-12 (R&D Systems) and transferred into recipient mice which were subsequently treated with pertussis toxin as previously described (Batten et al., 2006).

Flow cytometry. CNS-infiltrating cells were isolated as previously described (Batten et al., 2006). After incubation with anti-FcγRIII/II, cells were stained with antibodies to CLM-1, CD45, CD11b, and CD11c, fixed with 3% paraformaldehyde, resuspended in 0.1% Triton-X in PBS, and stained with 1 µg/ml rabbit anti-iNOS and PE-labeled donkey anti–rabbit IgG. For intracellular staining of TNF, cells were stimulated with 50 ng/ml PMA and 1 µM ionomycin in the presence of GolgiPlug (BD) and stained with anti-TNF antibody using the Cytofix/Cytoperm kit (BD) as per manufacturer's instruction. Intracellular staining of IL-17 and IFN-γ and T reg cell analysis was performed as previously described (Batten et al., 2006). Cells were analyzed using a FACSCalibur or LSRII flow cytometer (BD) and FlowJo software (Tree Star, Inc.).

Western blot analysis. BMDCs, generated as previously described (Inaba et al., 1992), were analyzed by immunoblotting with anti-CLM-1 antibody using standard methods.

Real-time PCR analysis. Total RNA from spinal cords was isolated using the RNeasy Protect Mini kit (QIAGEN) and complementary DNA synthesized using the High-Capacity cDNA Reverse Transcription kit (Applied Biosystems). CLM-1 mRNA and 18s ribosomal RNA were measured using the TaqMan Universal PCR Master Mix and verified primer and probe sets, Mm00467508_m1 and Hs03003631_g1, respectively (Applied Biosystems).

Cytokines. Cells isolated from spinal cords on day 15 as previously described (Batten et al., 2006) were cultured in RPMI1640 medium with and without MOG_{35-55} peptide. Cytokines in culture supernatants were measured by Luminex (Bio-Plex mouse 23-plex panel; Bio-Rad Laboratories). Nitric oxide production was measured using the Griess assay (Promega) according to the manufacturer's instructions. Ex vivo proliferation and cytokine responses were measured as previously described (Batten et al., 2006).

Immunohistochemistry. Anesthetized mice were transcardially perfused with PBS and 4% paraformaldehyde. Spinal cords were immersed in 40% sucrose and 7-µm thick sections were incubated with the following antibodies: anti-CLM-1 and biotin anti-CD45.2 followed by detection with Cy3 anti–hamster IgG and Alexa Fluor 488–streptavidin (Invitrogen), anti–CLM-1 and biotin anti-CD11c (HL3; BD) followed by detection with Cy3 anti–hamster IgG and Alexa Fluor 488–Streptavidin, and biotin anti-CD11c and goat anti MOG (R&D) followed by detection with Alexa Fluor 594–streptavidin (Invitrogen) and FITC donkey anti–goat antibodies. Sections were cover slipped with Prolong Gold anti-fade medium containing DAPI (Invitrogen) and examined in a fluorescent microscope (BX-61; Olympus). The area of demyelination was quantified using spinal cords stained with the FluoroMyelin staining kit (Invitrogen). Images were acquired using a BX-61 microscope at 40× final magnification and analyzed using the MetaMorph software package (MDS Analytical Technologies). Intensity thresholds and standard morphological filters were applied to identify large contiguous areas of demyelination. Results were expressed as total area of demyelination divided by the total area of myelination for each spinal cord cross section (Fig. S3 I).

Statistics. All p-values were calculated with an unpaired two-tailed Student's *t* test assuming equal variance.

Online supplemental material. Fig. S1 shows CLM-1 localization on CNS- and blood-resident inflammatory myeloid cells. Fig. S2 shows strategy of targeted disruption of the mouse *Clm-1* gene and expression analysis. Fig. S3 shows EAE incidence and demyelination in CLM-1 WT and KO mice. Fig. S4 shows that CLM-1 does not influence T cell responses. Online supplemental material is available at http://www.jem.org/cgi/content/full/jem.20091508/DC1.

We would like to acknowledge Ian Kasman, Jim Cupp, Wesley Chang, Lauri Diehl, Dimitry Danilenko, Wyne Lee, and Laszlo Komuves for their valuable contributions.

All authors except K.Y. Helmy and P.A. Wark are employees of Genentech Inc. The authors have no other conflicting interests.

Submitted: 13 July 2009
Accepted: 7 December 2009

REFERENCES

Alvarez-Errico, D., H. Aguilar, F. Kitzig, T. Brckalo, J. Sayós, and M. López-Botet. 2004. IREM-1 is a novel inhibitory receptor expressed by myeloid cells. *Eur. J. Immunol.* 34:3690–3701. doi:10.1002/eji.200425433

Alvarez-Errico, D., J. Sayós, and M. López-Botet. 2007. The IREM-1 (CD300f) inhibitory receptor associates with the p85alpha subunit of phosphoinositide 3-kinase. *J. Immunol.* 178:808–816.

Auffray, C., D.K. Fogg, E. Narni-Mancinelli, B. Senechal, C. Trouillet, N. Saederup, J. Leemput, K. Bigot, L. Campisi, M. Abitbol, et al. 2009a. CX_3CR1^+ $CD115^+$ $CD135^+$ common macrophage/DC precursors and the role of CX3CR1 in their response to inflammation. *J. Exp. Med.* 206:595–606. doi:10.1084/jem.20081385

Auffray, C., M.H. Sieweke, and F. Geissmann. 2009b. Blood monocytes: development, heterogeneity, and relationship with dendritic cells.

Annu. Rev. Immunol. 27:669–692. doi:10.1146/annurev.immunol.021908.132557

Bailey, S.L., B. Schreiner, E.J. McMahon, and S.D. Miller. 2007. CNS myeloid DCs presenting endogenous myelin peptides 'preferentially' polarize CD4+ T(H)-17 cells in relapsing EAE. *Nat. Immunol.* 8:172–180. doi:10.1038/ni1430

Batten, M., J. Li, S. Yi, N.M. Kljavin, D.M. Danilenko, S. Lucas, J. Lee, F.J. de Sauvage, and N. Ghilardi. 2006. Interleukin 27 limits autoimmune encephalomyelitis by suppressing the development of interleukin 17-producing T cells. *Nat. Immunol.* 7:929–936. doi:10.1038/ni1375

Benveniste, E.N. 1997. Role of macrophages/microglia in multiple sclerosis and experimental allergic encephalomyelitis. *J. Mol. Med.* 75:165–173. doi:10.1007/s001090050101

Can, I., S. Tahara-Hanaoka, K. Hitomi, T. Nakano, C. Nakahashi-Oda, N. Kurita, S. Honda, K. Shibuya, and A. Shibuya. 2008. Caspase-independent cell death by CD300LF (MAIR-V), an inhibitory immunoglobulin-like receptor on myeloid cells. *J. Immunol.* 180:207–213.

Chung, D.H., M.B. Humphrey, M.C. Nakamura, D.G. Ginzinger, W.E. Seaman, and M.R. Daws. 2003. CMRF-35-like molecule-1, a novel mouse myeloid receptor, can inhibit osteoclast formation. *J. Immunol.* 171:6541–6548.

Clark, G.J., X. Ju, C. Tate, and D.N. Hart. 2009. The CD300 family of molecules are evolutionarily significant regulators of leukocyte functions. *Trends Immunol.* 30:209–217. doi:10.1016/j.it.2009.02.003

Deshpande, P., I.L. King, and B.M. Segal. 2007. Cutting edge: CNS CD11c+ cells from mice with encephalomyelitis polarize Th17 cells and support CD25+CD4+ T cell-mediated immunosuppression, suggesting dual roles in the disease process. *J. Immunol.* 178:6695–6699.

Dogan, R.N., A. Elhofy, and W.J. Karpus. 2008. Production of CCL2 by central nervous system cells regulates development of murine experimental autoimmune encephalomyelitis through the recruitment of TNF- and iNOS-expressing macrophages and myeloid dendritic cells. *J. Immunol.* 180:7376–7384.

Fischer, H.G., and G. Reichmann. 2001. Brain dendritic cells and macrophages/microglia in central nervous system inflammation. *J. Immunol.* 166:2717–2726.

Fujimoto, M., H. Takatsu, and H. Ohno. 2006. CMRF-35-like molecule-5 constitutes novel paired receptors, with CMRF-35-like molecule-1, to transduce activation signal upon association with FcRgamma. *Int. Immunol.* 18:1499–1508. doi:10.1093/intimm/dxl083

Geissmann, F., S. Jung, and D.R. Littman. 2003. Blood monocytes consist of two principal subsets with distinct migratory properties. *Immunity.* 19:71–82. doi:10.1016/S1074-7613(03)00174-2

Hooper, D.C., O. Bagasra, J.C. Marini, A. Zborek, S.T. Ohnishi, R. Kean, J.M. Champion, A.B. Sarker, L. Bobroski, J.L. Farber, et al. 1997. Prevention of experimental allergic encephalomyelitis by targeting nitric oxide and peroxynitrite: implications for the treatment of multiple sclerosis. *Proc. Natl. Acad. Sci. USA.* 94:2528–2533. doi:10.1073/pnas.94.6.2528

Inaba, K., M. Inaba, N. Romani, H. Aya, M. Deguchi, S. Ikehara, S. Muramatsu, and R.M. Steinman. 1992. Generation of large numbers of dendritic cells from mouse bone marrow cultures supplemented with granulocyte/macrophage colony-stimulating factor. *J. Exp. Med.* 176:1693–1702. doi:10.1084/jem.176.6.1693

Izawa, K., J. Kitaura, Y. Yamanishi, T. Matsuoka, T. Oki, F. Shibata, H. Kumagai, H. Nakajima, M. Maeda-Yamamoto, J.P. Hauchins, et al. 2007. Functional analysis of activating receptor LMIR4 as a counterpart of inhibitory receptor LMIR3. *J. Biol. Chem.* 282:17997–18008. doi:10.1074/jbc.M701100200

Izawa, K., J. Kitaura, Y. Yamanishi, T. Matsuoka, A. Kaitani, M. Sugiuchi, M. Takahashi, A. Maehara, Y. Enomoto, T. Oki, et al. 2009. An activating and inhibitory signal from an inhibitory receptor LMIR3/CLM-1: LMIR3 augments lipopolysaccharide response through association with FcRgamma in mast cells. *J. Immunol.* 183:925–936. doi:10.4049/jimmunol.0900552

King, I.L., T.L. Dickendesher, and B.M. Segal. 2009. Circulating Ly-6C+ myeloid precursors migrate to the CNS and play a pathogenic role during autoimmune demyelinating disease. *Blood.* 113:3190–3197. doi:10.1182/blood-2008-07-168575

Márquez, J.A., E. Galfré, F. Dupeux, D. Flot, O. Moran, and N. Dimasi. 2007. The crystal structure of the extracellular domain of the inhibitor receptor expressed on myeloid cells IREM-1. *J. Mol. Biol.* 367:310–318. doi:10.1016/j.jmb.2007.01.011

Miller, S.D., E.J. McMahon, B. Schreiner, and S.L. Bailey. 2007. Antigen presentation in the CNS by myeloid dendritic cells drives progression of relapsing experimental autoimmune encephalomyelitis. *Ann. N. Y. Acad. Sci.* 1103:179–191. doi:10.1196/annals.1394.023

Serbina, N.V., T.P. Salazar-Mather, C.A. Biron, W.A. Kuziel, and E.G. Pamer. 2003. TNF/iNOS-producing dendritic cells mediate innate immune defense against bacterial infection. *Immunity.* 19:59–70. doi:10.1016/S1074-7613(03)00171-7

Shi, L., K. Luo, D. Xia, T. Chen, G. Chen, Y. Jiang, N. Li, and X. Cao. 2006. DIgR2, dendritic cell-derived immunoglobulin receptor 2, is one representative of a family of IgSF inhibitory receptors and mediates negative regulation of dendritic cell-initiated antigen-specific T-cell responses. *Blood.* 108:2678–2686. doi:10.1182/blood-2006-04-015404

Sunnemark, D., S. Eltayeb, M. Nilsson, E. Wallström, H. Lassmann, T. Olsson, A.L. Berg, and A. Ericsson-Dahlstrand. 2005. CX3CL1 (fractalkine) and CX3CR1 expression in myelin oligodendrocyte glycoprotein-induced experimental autoimmune encephalomyelitis: kinetics and cellular origin. *J. Neuroinflammation.* 2:17. doi:10.1186/1742-2094-2-17

Yu, X., K. Harden, L.C. Gonzalez, M. Francesco, E. Chiang, B. Irving, I. Tom, S. Ivelja, C.J. Refino, H. Clark, et al. 2009. The surface protein TIGIT suppresses T cell activation by promoting the generation of mature immunoregulatory dendritic cells. *Nat. Immunol.* 10:48–57. doi:10.1038/ni.1674